Selective Area Chemical Vapor Deposition of Aluminum Using Dimethylethylamine Alane

Michael G. Simmonds,† Isabelle Taupin,‡ and Wayne L. Gladfelter*,†

Department of Chemistry, University of Minnesota, Minneapolis, Minnesota 55455, and Elf Atochem, King of Prussia, Pennsylvania 19406

Received December 21, 1993. Revised Manuscript Received April 28, 1994®

Dimethylethylamine alane (DMEAA) was used to deposit Al films selectively on a variety of metal surfaces (Au, Ti, NiCr, W) in the presence of SiO_2, Si, and Si_3N_4. Selectivity (${}^{gs}S_{ns}$) was quantified as $(\theta_{gs} - \theta_{ns})/(\theta_{gs} + \theta_{ns})$ where θ_{gs} and θ_{ns} represent the coverage of the growth and non-growth surfaces, respectively. At 100 °C, Al films were deposited on 3-μm-wide Au strips in the presence of SiO_2 with excellent selectivity (${}^{Au}S_{SiO_2} > 0.99$). Extended deposition times or increased substrate temperatures led to a reduction in selectivity. At 180 °C selectivity dropped to zero. Removing the carrier gas (H_2) and decreasing the DMEAA partial pressure in the system had no significant effect. Encroachment, in which Al at the edges of the Au regions grew laterally onto adjacent SiO_2 strips, was observed and had a significant impact on the selectivity of a deposition. Even after very short DMEAA exposure times, trace amounts of Al were detected on silicon oxide surfaces using X-ray photoelectron spectroscopy. Pretreatment of the non-growth surface with hexamethyldisilazane, which converted surface OH groups on SiO_2 to trimethylsilyl ethers, did not enhance selectivity.

Introduction

Metal films are used in a variety of commercial applications and are produced mainly by evaporation and sputtering techniques. The potential advantages of chemical vapor deposition (CVD), such as conformal coverage and high throughput, have given rise to a sustained interest in its development for metal film deposition.[1,2] One of the most challenging goals in the area of CVD is to control a process so that the metal film is deposited selectively on one type of surface in the presence of different surfaces exposed to the same nominal precursor flux. Such a process would have the advantage of reducing the number of lithographic steps required for production of a device. The CVD literature describing the selective metallization of W, Al, and Cu thin films has recently been reviewed.[3]

A significant body of literature[4] exists which describes the deposition of Al films from a variety of molecular precursors molecules, most of which have exhibited some degree of selectivity. In general, these molecules deposit Al preferentially onto metallic surfaces in the presence of surfaces of insulators or semiconductors.

Tertiary amine complexes of alane (AlH_3) are able to deposite pure Al films at high deposition rates,[5-10] and initial reports of selectivity have appeared. Trimethylamine alane (TMAA) was found to deposit Al films at surface temperatures of around 100 °C preferentially on W lines patterned on a Si wafter,[11] and dimethylethylamine alane (DMEAA) deposited Al selectively on a Au film which had been evaporated onto a masked Si(100) wafer.[12] The current study builds on this initial finding and presents an appraisal of selective deposition using DMEAA. At different substrate temperatures and DMEAA partial pressures, selective deposits were obtained on a variety of metal surfaces in the presence of SiO_2, Si, and Si_3N_4. Some intriguing effects of the substrate pattern design and use of a surface pretreatment agent are also reported.

Throughout this paper, selectivity is defined as ${}^{gs}S_{ns}$ (eq 1),[3] where θ_{gs} and θ_{ns} are the fractional surface coverages of Al on the growth and non-growth surfaces, respectively.

$$ {}^{gs}S_{ns} = (\theta_{gs} - \theta_{ns})/(\theta_{gs} + \theta_{ns}) \quad (1) $$

A detailed discussion of the relationship between coverage and the rate of nucleation has been presented elsewhere.[3] It is critical to point out that selectivity, as defined in eq 1, provides a valuable empirical parameter for comparing depositions. It does not represent a fundamental constant, and selectivities will be expected to change during the course of a deposition. Scanning electron microscopy (SEM) in combination with Auger electron spectroscopy was used to evaluate θ_{gs} and θ_{ns}.

† University of Minnesota.
‡ Elf Atochem.
® Abstract published in *Advance ACS Abstracts*, June 1, 1994.

(1) Cooke, M. J. *Vacuum* **1985**, *35*, 67.
(2) Green, M. L.; Levy, R. A. *J. Metals* **1985**, *37*(6), 63.
(3) Gladfelter, W. L. *Chem. Mater.* **1993**, *5*, 1372.
(4) Simmonds, M. G.; Gladfelter, W. L. In *Chemical Aspects of Chemical Vapor Deposition for Metallization*; Kodas, T. T., Hampden-Smith, M. J., Eds.; VCH Publishers: New York, in press.
(5) Gladfelter, W. L.; Boyd, D. C.; Jensen, K. F. *Chem. Mater.* **1989**, *1*, 339.
(6) Gross, M. E.; Fleming, C. G.; Cheung, K. P.; Heimbrook, L. A. *J. Appl. Phys.* **1991**, 469, 2589.
(7) Beach, D. B.; Blum, S. E.; LeGoues, F. K. *J. Vac. Sci. Technol.* **1989**, *A7*, 3117.
(8) Baum, T. H.; Larson, C. E.; Jackson, R. L. *Appl. Phys. Lett.* **1989**, *55*, 1264.
(9) Wee, A. T. S.; Murrell, A. J.; Singh, N. K.; O'Hare, D.; Foord, J. S. *J. Chem. Soc., Chem. Commun.* **1990**, 11.
(10) Gross, M. E.; Cheung, K. P.; Fleming, C. G.; Kovalchick, J.; Heimbrook, L. A. *J. Vac. Sci. Technol.* **1991**, *A9*, 57.
(11) Houlding, V. H.; Coons, D. E. In *Tungsten and Other Advanced Metals for VLSI/ULSI Applications 1990*; Smith, G. C., Blumenthal, R., Eds.; Materials Research Society: Pittsburgh, 1990; p 203.
(12) Simmonds, M. G.; Phillips, E. C.; Hwang, J.-W.; Gladfelter, W. L. *Chemtronics* **1991**, *5*, 155.

0897-4756/94/2806-0935$04.50/0

Experimental Section

Substrates. Two kinds of substrates were used. One of these was a fine-line test pattern made from single-crystal Si wafers supporting a thermally grown amorphous SiO_2 (500 nm) layer (wafer type I). Using a standard lithographic procedure, strips of the SiO_2 were etched away and the underlying Si was coated with Cr (~15 nm) and then Au (30 nm) by evaporation. The width of the alternating Au and SiO_2 strips varied across a given wafer such that the smallest strips were 3 μm wide and the largest were 10^3 μm wide. Individual substrates were 6 × 6 mm. A second type of Si substrate measuring 10 × 10 mm had four different regions (wafer type II). Two of these regions were coated with a film of polycrystalline metal (100 nm) and the other two regions contained either Si_3N_4 (150 nm) or polysilicon (400 nm, heavily P doped). In regions with metal present, the metal had been coated onto half of the underlying Si_3N_4 and polysilicon surfaces. These metals were Ti (present as Ti and TiN), NiCr, W and Pt.

Substrate Preparation. Type I wafers were cleaned using the following procedure: After an initial immersion (6 min) in a 4:1 H_2SO_4 (98%):H_2O_2 (30%) aqueous solution to remove hydrocarbons, they were placed under a flow of deionized water (18.2 MΩ cm) for 4–5 min and dried in a N_2 stream. This was followed by dipping (2 min) the wafers in HF (0.5%) to etch away a thin layer (~3–4 nm) of the SiO_2, rinsing them in water, and drying them with a stream of N_2. The wafers were then left under a UV lamp in air (6 min) to remove the remaining surface adsorbed hydrocarbons[13] and were immediately transferred into the reactor. Type II wafers were used as received without additional cleaning.

The substrates were attached by a metal clip to a thin (<400 μm) Mo disk which in turn was placed over a hole in a stainless steel holder. The holder was transferred into the reactor via the load-lock and was positioned above a resistively heated tungsten filament. The filament was wound around a series of tungsten pins attached to a BN annulus (approximately 40-mm diameter) so that the heated area was greater than the dimension of the substrates. The entire assembly was housed inside a six-way stainless steel cross where Al films were deposited.

Temperature Calibrations. Wafer temperature calibrations were conducted under typical temperature, flow and pressure conditions using two 0.01-in. thermocouples (K type). For experiments where no carrier gas was used, the system was calibrated at the base pressure under a dynamic vacuum. The calibrations were performed by two methods. First, one of the thermocouples (always present) was spot welded to the heater edge, while the other (removable) was attached with the substrate clip to the substrate surface. This latter thermocouple was assumed to read the real substrate temperature and was used to calibrate the response of the thermocouple attached to the heater. In the second method, a thermocouple attached to a feedthrough directly above the substrate holder was calibrated against a thermocouple positioned on the substrate surface. The feedthrough was clamped to the six way cross using a rubber O-ring seal. Prior to a deposition, the moveable thermocouple was brought into contact with the wafer surfaces so that the wafer could be equilibrated to the desired temperature. During a deposition, it was placed in a cool region of the reactor so that the junction was not damaged. The relationship between the thermocouples was obtained with a precision of 2 °C and the wafer temperature at different positions on the surface varied by up to 2 °C.

Reactor Description. A schematic of the apparatus used to perform the Al depositions is shown in Figure 1. The main components of this cold wall CVD reactor were made of 6.5-cm outer-diameter stainless steel tubing using knife edge seals for ultrahigh-vacuum (UHV) compatibility. The turbomolecular pump (150 L/s) used to evacuate the system led to a base pressure of 10^{-7} Torr. A separate turbomolecular pump evacuated the gas lines (6.5-mm outer-diameter stainless steel tubing) to a similar base pressure.

Precursor Preparation. Dimethylethylamine alane was synthesized using a literature procedure[12] and was purified by vacuum distillation during which the receiving vessel temperature was −20 °C. The liquid precursor (1–5 mL) was stored at room temperature in a stainless steel capped Pyrex vessel attached to the CVD system for periods of several months. Immediately before use it was degassed in one of two ways. The first method involved three freeze–pump–thaw degas cycles, and in the second an auxiliary mechanical vacuum pump was used to evacuate the precursor storage vessel continuously during use. A valve between the outlet of the vessel and the mechanical pump allowed the rate of pumping to be varied. This technique was used throughout the time that the precursor was passed into the reactor and was found to be more efficient than the freeze–thaw method. It did, however, consume more precursor.

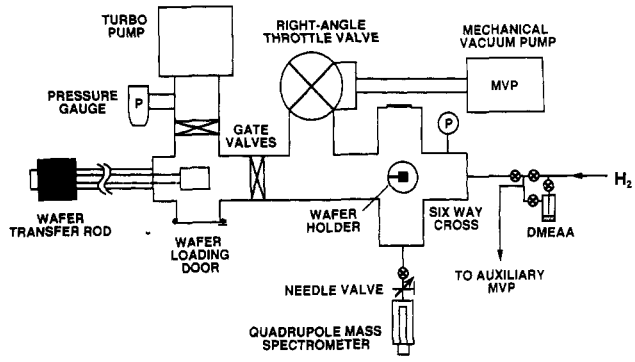

Figure 1. Schematic of the cold-wall low-pressure CVD system used to deposit Al films.

The pressures of DMEAA and H_2 in the gas phase in the reactor were monitored continuously using a Leybold Inficon quadrex 200 quadrupole mass spectrometer using the ion current signals at m/e 102 and 2, respectively. Smaller quantities of the precursor were sometimes found to pass into the reactor when the storage vessel was first opened. This was attributed to some decomposition of the precursor in the storage vessel at ambient temperatures. The best results were obtained when the precursor storage vessel was dynamically evacuated with the auxiliary mechanical pump while simultaneously flowing the DMEAA vapors into the reactor. This procedure allowed stable ion current signals to be routinely monitored and was especially valuable for leaking DMEAA into the reactor at alow pressures (10^{-4}–10^{-5} Torr). These observations emphasized the need for the degassing procedures before running a deposition.

Depositions in Hydrogen. Once the base pressure had been reached, Pd-purified H_2 was introduced into the reactor at a rate of 100 sccm with the assistance of a mechanical vacuum pump fitted with a Micromaze foreline trap (Figure 1). A capacitance manometer enabled the pressure in the six-way cross to be monitored and adjustments to the pressure were made with the right angle valve. Upon initiation of the flow of H_2 through the reactor, the wafer was heated. Typically, 30 min were required for the temperature to equilibrate. Once at 3.0 Torr and the appropriate substrate temperature, the flow of H_2 was diverted through the precursor storage vessel. The pressure in the deposition region typically increased to 3.3–3.4 Torr. Effluents from the CVD process were safely eluted to a fume hood via a cracking furnace and a 10-μm particle filter. The furnace, which was at 700 °C, was used to consume unreacted alane before it reached the mechanical pump. After the desired processing time had elapsed, the H_2 flow was diverted around the precursor vessel and the system was flushed for 10 min prior to its evacuation and wafer removal. Depositions were conducted at substrate temperatures in the range 100–200 °C.

Hexamethyldisilazane Modification. Hexamethyldisilazane (HMDS) was stored on a separate gas line on the reactor which was identical that to which the precursor was attached. Silicon dioxide surfaces were pretreated[14] with the HMDS prior to the flow of DMEAA by allowing the HMDS vapor to equilibrate in the reactor to its room-temperature vapor pressure (~12 Torr)

(13) Zazzera, L. A.; Evans, J. F. *J. Vac. Sci. Technol.* **1993**, *A11*, 934.

(14) Zazzera, L. A.; Tirrell, M.; Evans, J. F. In *Polymer/Inorganic Interfaces*; Opila, R. L., Boreo, F. J., Czanderna, A. W., Eds.; Materials Research Society: Pittsburgh, 1993; p 125.

over 45–60 min. During this time, the heater was turned off. The substrate temperature, which was initially 180 °C, therefore decreased to a final value which was close to room temperature. HMDS vapor in the reactor, along with products of the pretreatment, were removed with the mechanical pump before equilibrating the system in a flow of H_2.

Depositions without Hydrogen. With the system at the base pressure and with the substrate equilibrated to the desired deposition temperature, the precursor was leaked into the reactor. A combination of the turbomolecular pump depicted in Figure 1 and a gas-regulating valve on the outlet of the precursor vessel enabled depositions to be performed at pressures of 2.5×10^{-4} and 2.5×10^{-5} Torr according to uncorrected ion gauge readings. Aluminum films were grown on Au/SiO_2 wafers at a temperature of 100 °C for 3.5 h. A calibration using a mass flow controller to deliver H_2 at the same ion gauge reading suggested that the DMEAA flux through the reactor at 2.5×10^{-4} Torr was similar to the DMEAA flux at a total pressure of 3.3–3.4 Torr. Although consideration was given to the different pumping speeds of H_2 and DMEAA with the turbo pump, the difference in the sensitivity of the ion gauge to the different gases was not known and was therefore assumed to be zero.

Analysis of CVD Processed Wafers. Before and after CVD processing, the substrate morphologies were assessed with a Hitachi S900 SEM operating at 10-kV accelerating voltage. The microscope was fitted with an Antrata type single-crystal YAG backscatter detector. Cross-sectional views of the wafers with this microscope were used to determine the Al film thicknesses and image analysis of plan views allowed the Al coverages on the different substrate surfaces to be calculated. The digitized images were captured with a SPARC Sunstation IPC using Visilog software (version 4.1) from Noesis (France) and a Pulnix camera. Selectivity was calculated according to eq 1.

X-ray photoelectron spectroscopic (XPS) data were collected on a Perkin-Elmer PHI 5400 small area instrument operating with a hemispherical electrostatic electron energy analyzer. Analysis was made with Mg Kα radiation at 300 W of power with a pass energy of 35 eV. The experimental resolution was measured at 1 eV with the Ag 3d emission and electron binding energies were calibrated against the Au $4f_{7/2}$ peak at 84.0 eV. Auger data were recorded with a Perkin-Elmer PHI 595 SAM system at a primary beam energy of 3 or 5 keV. At a primary beam current of 150 nA, the beam could be focused to a diamer of 0.5–1 μm and line scans were obtained with a lateral resolution of about 1 μm. For general elemental surveys, a 100×100 μm rectangle was analyzed in scanning mode. Elements were detected to atomic concentrations of 1%.

Results

(A) Depositions Using Type I Wafers. *Depositions at 100 °C.* Depicted in Figure 2 in a SEM of 3-μm-wide au and SiO_2 strips present on a fine-line test pattern. After 4 min of exposure to DMEAA in a flow of H_2 and at a substrate temperature of 100 °C the Au regions had lost their characteristic color and were highly reflective. Comparison of the surface morphologies with SEM before and after processing indicated that a continuous film had deposited on the Au. A granular structure with an Al grain size of ~80 nm was observed (Figure 3A). In contrast, the surface of the SiO_2 strips appeared featureless even when examined at high magnification (150 K). A micrograph of the wafer edge (Figure 3B) verified the presence of a thin Al deposit (~30 nm) on top of the Au surface.

In Figure 2, the results of an Auger line scan across the wafer have been superimposed onto the SEM background of the same region. The line scan in which the Al, Au, and Si signal intensities were simultaneously monitored verified that Al was present on the Au strips. No Au substrate peak was detected. A spot analysis of the SiO_2 surface did lead to the detection of trace amounts of Al. Ignoring these trace quantities, the selectivity of the deposit for Au was >0.99.

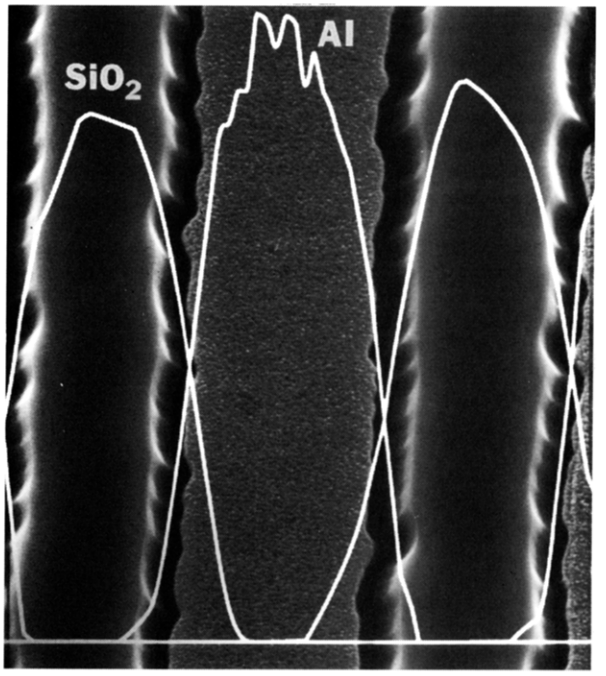

Figure 2. SEM of the Au/SiO_2 fine-line test pattern exhibiting 3-μm-wide au and SiO_2 strips after exposure to DMEAA at 100 °C for 4 min. The partial pressure of H_2 was 3.0 Torr and the total system pressure was 3.3–3.4 Torr. Superimposed onto the SEM are the results of an Auger line scan across the test pattern in which the Al (1378 eV), Au (239 eV) and Si (76 eV) signal intensities were simultaneously monitored. The primary electron beam energy was 5 keV. Al selectively grew on Au.

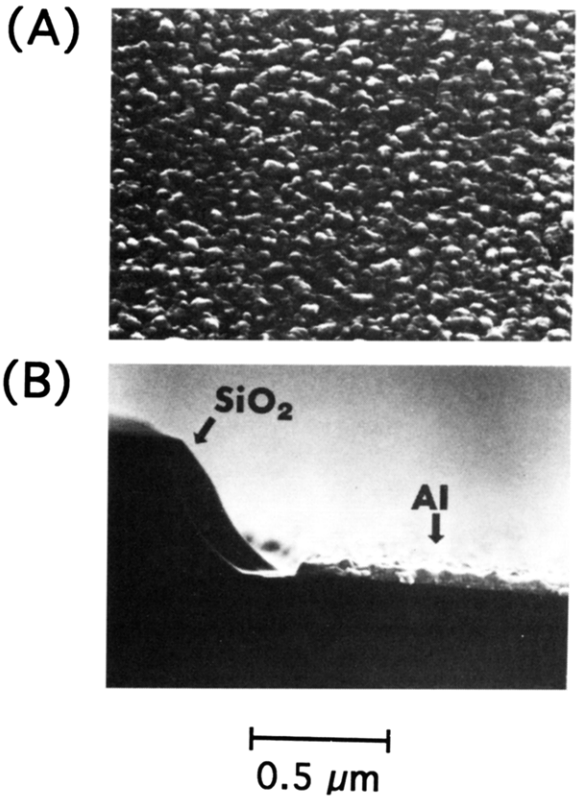

Figure 3. (A) Morphology of the Al film on Au. (B) Cross-sectional view of the Au/SiO_2 test pattern shown in Figure 2 depicting a thin layer of Al on top of a Au strip.

Effects of Substrate Temperature, Deposition Time, and Pressure. Figure 4 shows the surface of two Au/SiO_2

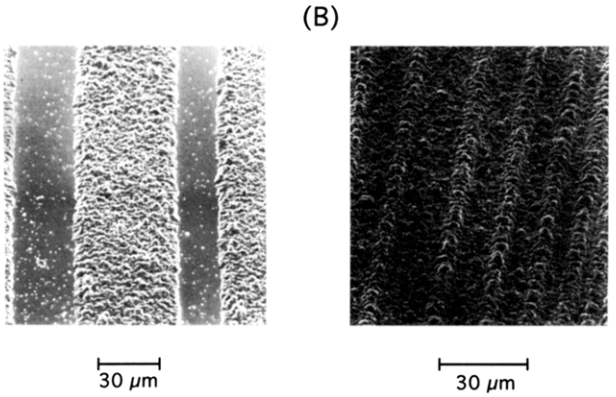

Figure 4. Effect of increasing the Au/SiO_2 wafer temperature. Wafer B ($^{Au}S_{SiO_2}$ = 0.65) was at a temperature of 160 °C and wafer C ($^{Au}S_{SiO_2}$ = 0) was at 200 °C. The deposition time in both cases was 4 min. For the wafer processed at 160 °C, selectivity was computed from a magnified view of the SiO_2 surface. In each case, the samples were tilted at an angle of 40° for imaging.

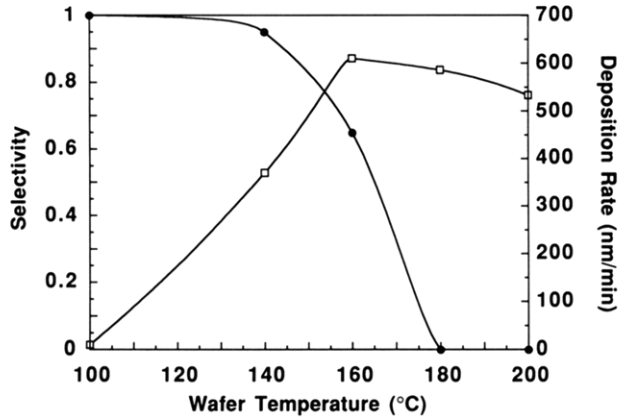

Figure 5. Summary of Al selectivity and Al growth rate on Au as a function of wafer temperature. All of the wafers (Au/SiO_2 test patterns) were exposed to DMEAA for 4 min in a flow of H_2.

wafers which were processed at substrate temperatures of 160 and 200 °C for 4 min in a flow of DMEAA and H_2. At 160 °C, Al particles were evident on the SiO_2 surface while a rough continuous Al film had grown on the Au. The selectivity of this deposition was 0.65. Films deposited at 200 °C totally covered both the Au and SiO_2 regions ($^{Au}S_{SiO_2}$ = 0). Figure 5 summarizes the selectivities and growth rates observed in the temperature range 100–200 °C. Between 160 and 200 °C the films grew at a similar rate of 530–610 nm/min, suggesting that their growth was limited by the supply of precursor to the surfaces. Because the wafer holder was substantially larger than the wafers, the slight decreasing trend in the growth rate in this temperature range is believed to be the result of the precursor becoming depleted at the leading edge of the wafer holder. Depletion effects with DMEAA were also noticed in a related hot-wall system operated under similar deposition conditions.[12]

Examination in cross section of a wafer processed at a temperature of 160 °C established that Al had encroached over the Au/SiO_2 boundaries onto the SiO_2. Figure 6 shows the effect of the overgrowth on the assessment of selectivity for the deposition. Micrographs A and B are the edge views showing SiO_2 strips which are 16 μm (A) and 3 μm (B) wide. The 16-μm-wide SiO_2 strip was wider than twice the lateral overgrowth distance (5 μm). Assessing the selectivity of the deposition based only on the Al particles in this region of the wafer yielded a value of 0.98. Because the 3-μm-wide strips were narrower than the overgrowth distance, the SiO_2 strips were completely covered with Al.

At longer DMEAA exposure times and with wafers at 100 °C, the extent of selectivity was eventually diminished. After 40 min, for example, the selectivity dropped to 0.96. The thickness of the film on Au after 40 min was 800 nm leading to a growth rate of 20 nm/min. Under these conditions aluminum had once again encroached over the Au/SiO_2 boundaries so that SiO_2 strips which were 3 μm wide were completely covered. Nonuniformities in the distribution of the Al particles at the edges of the SiO_2 strips were observed over large regions. In some places, the particles had accumulated preferentially at the edges of the overgrowth region described above. In other places, the effect was reversed so that smaller numbers of Al particles were observed. The latter effect is illustrated in the section describing the effects of HMDS pretreatment. Temperature increases (up to 15 °C) above 100 °C occurred at these long exposure times because of the heating system design.

Aluminum films grown at 10^{-4} and 10^{-5} Torr at 100 °C also selectively deposited onto Au (grain size > 1000 nm). From a film thickness of 2 μm, the growth rate on Au at 10^{-4} Torr was 10 nm/min, and the selectivity was 0.98. Aluminum at the Au/SiO_2 boundaries had encroached over the edges of the SiO_2 strips by 3.5 μm.

Effects of HMDS Modification. Hexamethyldisilazane was used to pretreat the surface of wafers processed at 100 and 160 °C. No enhancement in the extent of selectivity relative to untreated wafers was noticed. Figure 7 shows the surface of a wafer which had been pretreated with HMDS at 100 °C and exposed to DMEAA for 25 min under the same conditions as the wafer shown in Figure 2. Micrograph A is a low-magnification plane view of the Au and SiO_2 strips after processing. Rough Al films (600-nm grain size) had grown on Au, and the extent of selectivity was considerably diminished as assessed by the variety of faceted particles present on SiO_2. Highlighted in micrograph B are the morphologies of these particles, and on the basis of an analysis of the region defined only by the Al particles, the selectivity of the process was 0.69. Cross sections of the wafer again indicated that Al had overgrown from the Au region onto the edges of the SiO_2 strips. Adjacent to the Al growth front on the SiO_2 region, Figure 7 displays a distinct zone (approximately 1 μm in width) that is depleted of aluminum particles. When the SiO_2 strips were thin, as in the case of the 3-μm-wide lines, the selectivity was significantly enhanced due to this effect. This is demonstrated on the thin lines in Figure 7A.

(B) Depositions Using Type II Wafers. These wafers were processed at a temperature of 100 °C for 6 min under the same pressure and flow conditions typically used for type I wafers. The surfaces on a wafer supporting a Ti film before and after CVD processing are compared in Figure 8 which shows that Al grew selectively on the Ti regions. Some Al particles were found on Si and Si_3N_4 such that the selectivities ($^{Ti}S_{SiO_2}$ and $^{Ti}S_{Si_3N_4}$) were 0.96 (the Al coverage for the growth surface was defined by the Ti-coated-on-Si region). Figure 8 also shows that the morphologies of the Al films deposited on the Ti-coated-on-Si region (lower left quadrant) and Ti-coated-on-Si_3N_4 region (lower right quadrant) are different. It was common to observe morphological differences between the Al deposited on metal-surfaces-coated-on-Si and metal-surfaces-coated-on-Si_3N_4. The former films usually ap-

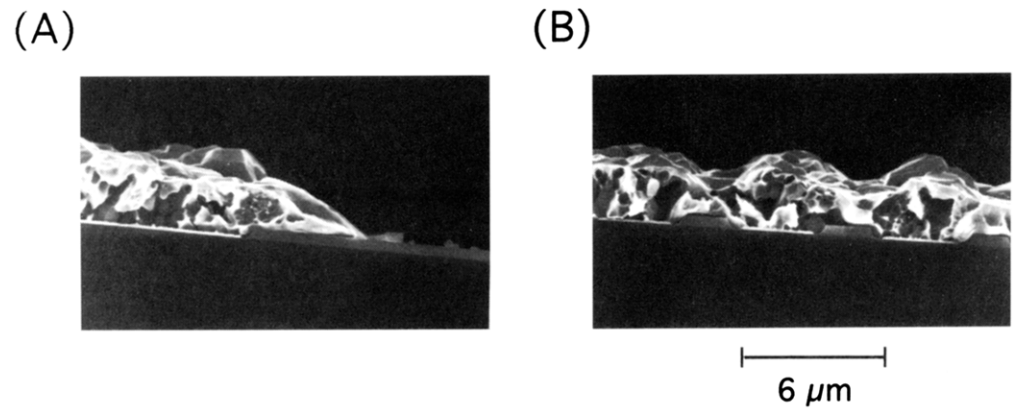

Figure 6. Cross-sectional views of a Au/SiO_2 test pattern showing the effect of the SiO_2 strip width on the assessment of selectivity. The SiO_2 strip in micrograph A is 16 μm wide, which is greater than twice the encroachment width. Aluminum selectively grew on Au. The strips in micrograph B (3 μm) are narrower than the encroachment wiedth and are therefore completely covered with Al. This wafer had been processed for 4 min at 160 °C in a flow H_2.

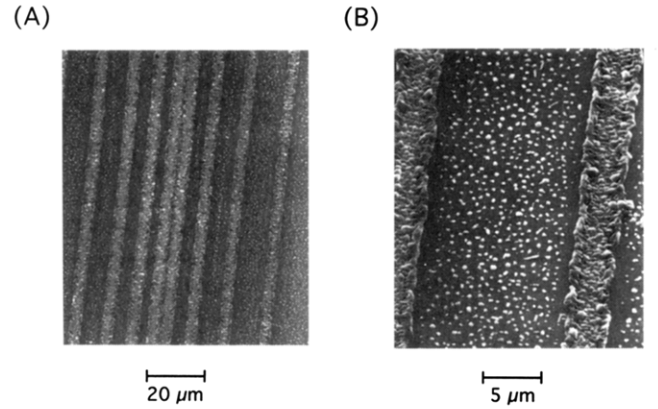

Figure 7. Plan views of a Au/SiO_2 test pattern which had been pretreated with HMDS before exposure to DMEAA and H_2 for 25 min. The wafer temperature was 100 °C. Micrograph A is an overview of the substrate surfaces showing the distribution of Al particles on SiO_2 strips having varying widths. Micrograph B highlights the faceted morphology of these Al particles as well as the nonuniform distribution of Al in the Au/SiO_2 boundary regions. The sample was tilted by 40° for imaging.

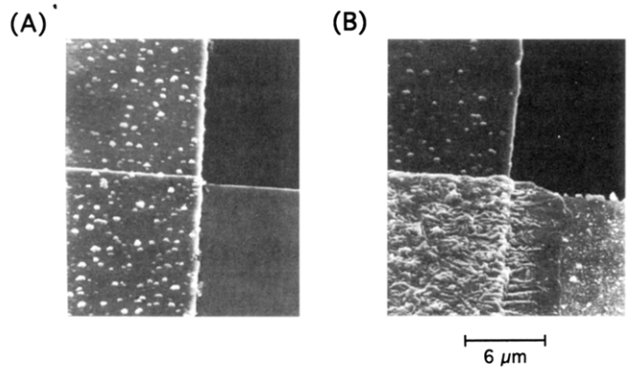

Figure 8. Scanning electron micrographs of two type II test patterns showing the selectivity of DMEAA for depositing Al on Ti in the presence of Si and Si_3N_4. The four regions on the test patterns are Si (upper left), Si_3N_4 (upper right), Ti coated on Si (lower left), and Ti coated on Si_3N_4 (lower right). Micrograph A shows the starting surfaces and micrograph B shows the result of exposing the test pattern at around 100 °C to DMEAA vapor for 6 min in a flow of H_3 (3.0 Torr). The total system pressure was 3.3 Torr. These wafers were imaged at a tilt angle of 40°.

peared to have larger grains and a more uniform structure, while the latter contained a variety of crystallite sizes and shapes including numerous whiskers.

Rough Al deposits also selectively grew on TiN, NiCr, and W surfaces. Curiously, the morphology of the Pt surface was unchanged after processing according to SEMs recorded up to a magnification of 250 K. Auger spectroscopy did, however, lead to the detection of Al as well as Pt on these wafers, indicating that only a few layers of Al were present. Cleaning the surface of a Pt substrate by Ar ion sputtering in a separate vacuum chamber before processing had no effect on the deposition.

When the three different boundary regions on the wafer supporting Ti were examined, the results shown in Figure 9 were obtained. These regions were comprised of Ti-coated-on-Si and Ti-coated-on-Si_3N_4 (A), Ti-coated-on-Si_3N_4 and Si_3N_4 (B), and Si- and Ti-coated-on-Si (C). In two of the boundary regions (A and B), Al had grown more rapidly than expected and had encroached over the boundaries onto the Ti-coated-on-Si_3N_4 (A) and Si_3N_4 regions (B). For the third case (C), Al in the boundary region had grown at the same rates as at positions further away from the boundary. The border regions shown in Figures 8B and 9A,B exhibit unusual morphologies of the Al. In each case the deposit appears as if it is growing away from the step down from the higher (growth) level to the lower (nongrowth) level. This effect could be caused by the vertical wall of the growth surface. In the case of the border illustrated in Figure 9C, the lack of excess overgrowth might be due to a reduced sticking coefficient of the precursor on silicon or possibly a diminished ability of aluminum to wet the silicon surface.

Surface Analysis of Substrates. At an electron takeoff angle of 15 or 45°, and using standard Gaussian/Lorentzian curve-fitting routines and tables, the metals Ni, Cr, Ti, and W were found to exhibit XPS peaks at binding energies characteristic of both the metal oxides and the metallic states. In contrast, Pt and Au surfaces gave rise to signals which identified the presence of only the metallic states. Oxygen was detected on the surface of both Si and Si_3N_4 by Auger electron spectroscopy.

Figure 10 shows XPS data recorded from silicon oxide surfaces which had been exposed to DMEAA in a flow of H_2 for (I) 15 s at 100 °C and (II) 600 s at 100 °C. The ratio of the integrated Al(2p) and Si(2p) signals have been plotted as a function of the electron takeoff angles and illustrate the presence of small amounts of Al on silicon oxide, even after a very short exposure time. A substantial increase in the exposure time, however, gave rise to only a small increase in the amount of Al detected.

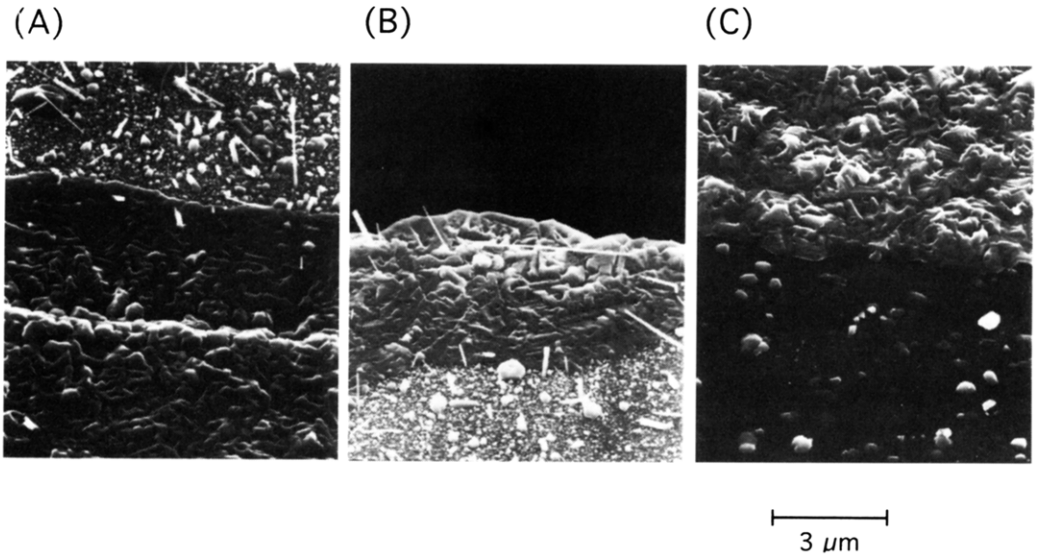

Figure 9. Plane views showing the distribution of Al at the three boundary regions on the test pattern depicted in Figure 8. These regions comprised of Ti-coated-on-Si (bottom) and Ti-coated-on-Si_3N_4 (top) (A), Ti-coated-on-Si_3N_4 (bottom) and Si_3N_4 (top) (B), and Si (bottom) and Ti-coated-on-Si (top) (C).

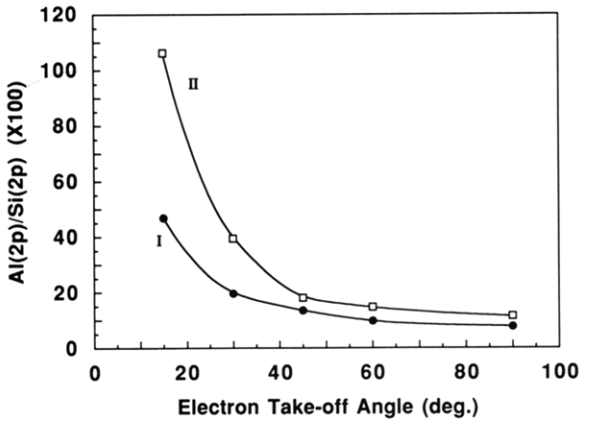

Figure 10. X-ray photoelectron spectroscopic data recorded from silicon oxide surfaces (100 °C) which had been exposed to DMEAA in a flow of H_2 for (I) 15 and (II) 600 s. The partial pressure of H_2 was 3.0 Torr, and the total reactor pressure was 3.3–3.4 Torr. The ratio of the integrated Al(2p) (76 eV) and Si(2p) (100 and 104 eV) signals have been plotted as a function of the electron takeoff angles. Small quantities of Al deposited on silicon oxide, even after a very short exposure time.

Discussion

The present study demonstrates that DMEAA could deposit Al readily on most metallic surfaces but not on SiO_2, Si_3N_4, or Si. At a substrate temperature of 100 °C and a 4-min DMEAA exposure time, Al was deposited on Au with nearly perfect selectivity (${}^{Au}S_{SiO_2} > 0.99$). At longer exposure times (40 min) the extent of selectivity dropped off significantly (${}^{Au}S_{SiO_2} = 0.96$). As the temperature was raised above 140 °C, the selectivity dropped rapidly, and by 180 °C the process was unselective (${}^{Au}S_{SiO_2} = 0$). Decreasing the partial pressure of DMEAA in the system by several orders of magnitude and removing the H_2 had no effect on selectivity. The thickness of the film is a product of the growth rate and time, and during this study we have focused on these two parameters separately. In future studies, we plan to correlate selectivity directly with film thickness.

Preference for Deposition on Metallic Surfaces. Although the mechanism of DMEAA decomposition on Au has not been investigated, the decomposition mechanisms of TMAA and triethylamine alane on single-crystal surfaces of Al have been studied under UHV conditions.[15,16] The ultimate source of electrons for the deposition of the Al comes from the reductive elimination of hydrogen from the surface. This may help to explain the facile growth of Al from amine–alane adducts on Au and other metallic surfaces. When the precursor adsorbs on the metals, hydrogen atoms are dispersed over the surfaces and H_2 loss is able to occur under relatively mild conditions. Hydrogen desorption is known to occur from clean, annealed, polycrystalline Au surfaces at around −60 °C.[17] The difficulty in nucleating Al on SiO_2 is probably related to the inability of H atoms to desorb readily as H_2. In the absence of a mechanism to reduce the aluminum, nucleation cannot occur readily. This higher barrier for nucleation on SiO_2 compared to metals is the cause of selectivity.

Selectivity Loss. The fact that aluminum does eventually deposit on SiO_2 means that an alternative mechanism for nucleation is available. To probe the nature of this alternative, we examined the interaction that occurs between DMEAA and SiO_2. X-ray photoelectron spectroscopy of substrates that were removed from the reactor and transported in air to the analysis chamber established that some aluminum was present on the surface. The same differences in peak intensities between the 15- and 600-s second time of exposure to DMEAA suggest that the reactive sites saturate rapidly. Unfortunately, we could not meaningfully probe the oxidation state of the aluminum because the sample was exposed to air. Electron spectroscopy results with trimethylamine alane (TMAA) suggest that it can also adsorb on a thermally grown SiO_2 surface under UHV conditions in the intact molecular state.[18]

In a separate surface infrared study in which the interactions between DMEAA and a hydrated, thin oxide

(15) Dubois, L. H.; Zegarski, B. R.; Kao, C.-T.; Nuzzo, R. G. *Surf. Sci.* **1990**, *236*, 77.
(16) Dubois, L. H.; Zegarski, B. R.; Gross, M. E.; Nuzzo, R. G. *Surf. Sci.* **1991**, *244*, 89.
(17) Lisowski, E.; Stobinski, L.; Dus, R. *Surf. Sci.* **1987**, *188*, L735.
(18) Elms, F. M.; Lamb, R. N.; Pigram, P. J.; Gardiner, M. G.; Wood, B. J.; Raston, C. L. *J. Chem. Soc., Chem. Commun.* **1992**, 1423.

layer on SiO_2 were investigated, more detailed information was discovered.[19] Under typical CVD conditions, DMEAA was found to bind to the surface via strong Al–O bonds formed following the loss of H_2 from the reaction with surface OH groups. The presence of these species accounts for the trace quantities of Al detected by XPS on SiO_2 in this study. The immobile nature of the Al centers in these species may also inhibit clustering which is thought to be a necessary step for growth. These results resemble those obtained when triisobutylaluminum was adsorbed on silicon oxide (a surface on which growth did not readily occur).[20] Aluminum atoms on the surface formed strong Al–O bonds and were thought to retain a single isobutyl ligand, even above typical growth temperatures. The presence of this layer passivated the surface toward adsorption of fresh precursor.

The search for the cause (or causes) of nucleation on the non-growth surface is complicated because it occurs very infrequently compared to deposition on the growth surface. The formation of unique products or a spectroscopic signature during nucleation on the non-growth surface is usually lost in the noise of the experiment. Outlined below are observations that suggest a relationship between the loss of selectivity and the presence of two species: water and silicon hydrides.

In a recent investigation, intentional introduction of trace quantities of H_2O into the CVD reactor induced the formation of metallic Al particles in the gas phase from DMEAA.[21] In contrast, introduction of similar quantities of O_2 gave rise to aluminum oxide particles. During the current study, trace quantities of H_2O were present in the gas phase of our CVD reactor as well as adsorbed on the surface of SiO_2. It is possible that these sources of H_2O lead to Al nuclei formation which were ultimately responsible for the loss of selectivity. This could occur in the gas phase or on the SiO_2 surface. The infrared study confirmed that *adsorbed* H_2O and surface silanols (SiOH) were consumed when DMEAA was exposed to silicon oxide surfaces.

Hydroxyl groups present on the surface of silicon oxide have been implicated as being at least partially responsible for the loss of selectivity in Cu CVD processes. Treating silicon oxide surfaces with $(CH_3)_3SiCl$ has been successful in enhancing the degree of Cu selectivity.[22] This molecule is thought to hydrogen bond to surface hydroxyls thereby inhibiting their reactivity toward Cu precursors. In the current study, the effect on selectivity of reacting the surface OH groups with HMDS was investigated. Hexamethyldisilazane has been used for some time to passivate the surface of silica packings used in chromatography columns, and its success is attributed to a reaction which converts OH groups present on silica surfaces to $OSi(CH_3)_3$ groups.[23] The $[-O_3SiOSi(CH_3)_3]$ species formed in our system did not lead to an enhancement in selectivity at a substrate temperature of 160 °C where selectivity without pretreatment was also found to be poor. This is consistent with the observation in the infrared study that HMDS pretreatments did not significantly effect DMEAA reaction on silicon oxide at a similar temperature.[19]

During the infrared spectral study, a distinct silicon–hydride stretch was observed especially when the substrate temperature was 145 °C. As shown in Figure 5, this corresponds to the temperature where loss of selectivity becomes rapid, and we cannot overlook a possible cause-and-effect relationship between these observations. The presence of Si–H groups on HF treated Si surfaces are thought to be critical to the deposition of Al from dimethylaluminum hydride.[24]

Although we can suggest the relationship between these observations and the loss of selectivity, there are no effective molecular models that are available to help us understand how H_2O or SiH moieties could induce nucleation of aluminum particles. One possibility is that these groups are capable of forming strong bridging interactions between two or more aluminum hydride fragments. For example, reaction of both protons on water with DMEAA could lead to an oxo-bridged dimer, $(Me_2EtN)AlH_2–O–AlH_2(NMe_2Et)$. Perhaps the close proximity of the aluminum hydride groups in such a molecule would promote the reductive elimination of H_2 with concomitant formation of an Al–Al bond. Subsequent addition of more alane groups and further elimination of hydrogen could lead to aluminum hydride clusters that may be intermediates on the way to metal particles.

Effect of Growth Surfaces. In view of the critical role of H_2 desorption expected in the growth of Al films, it is somewhat surprising that Al films could be grown on a variety of metal surfaces that are coated with a native metal oxide layer. Studies of the interactions between evaporated metal atoms and metal oxide surfaces have determined that the original oxide surfaces can be chemically reduced.[25–27] For example, Al atoms on TiO_2 led to the formation of reduced Ti centers as well as aluminum oxide, while Ni_3Al was formed when NiO surfaces were exposed to Al atoms.[26] In both cases, metallic regions of Al grew at greater coverages. The hydrides of Al are known to be powerful reducing agents and the formation of aluminum oxide adds a tremendous driving force for the reduction. Assuming that the metal oxides can be reduced by DMEAA, they, or the reduced products, could catalyze the nucleation of Al.

Lateral Al Thickness Uniformity. The results of this study have highlighted some intriguing observations in the boundary regions between the various growth and non-growth surfaces (Figures 6, 7, and 9). Aluminum, which had encroached onto SiO_2, was greater in width than the vertical thickness of the Al films on the Au regions. This suggests that the flux of the growth species at the edges of the growing films on Au was greater than the flux impinging on the surface of the films. Similar observations have been made for films deposited from other CVD systems, notably for epitaxial semiconducting films.[28–30] Gas-phase and/or surface diffusion play a critical role in determining the distribution of surface deposits. In the former case, the growth species are transported via a series

(19) Gladfelter, W. L.; Simmonds, M. G.; Zazzera, L. A.; Evans, J. F. In *Gas Phase and Surface Chemistry in Electronic Materials Processing*; Mountziars, T. J., Westmoreland, P. R., Smith, F. T. J., Paz-Pujalt, G. R., Eds.; Materials Research Society: Pittsburgh, in press.
(20) Mantell, D. A. *J. Vac. Sci. Technol.* **1991**, *A9*, 1045.
(21) Simmonds, M. G.; Gladfelter, W. L.; Li, H.; McMurry, P. H. *J. Vac. Sci. Technol.* **1993**, *11*, 3026.
(22) Jain, A.; Farkas, J.; Kodas, T. T.; Chi, K. M.; Hampden-Smith, M. J. *Appl. Phys. Lett.* **1992**, *61*, 2662.
(23) Hertl, W.; Hair, M. L. *J. Phys. Chem.* **1971**, *75*, 2181.
(24) Tsubouchi, K.; Masu, K. *Thin Solid Films* **1993**, *228*, 312.
(25) Dake, L. S.; Lad, R. J. *Surf. Sci.* **1993**, *289*, 297.
(26) Imaduddin, S.; Lad, R. J. *Surf. Sci.* **1993**, *290*, 35.
(27) Diebold, U.; Pan, J.-M.; Madey, T. E. *Surf. Sci.* **1993**, *287/288*, 896.
(28) Bhat, R. *J. Cryst. Growth* **1992**, *120*, 362.
(29) Yamaguchi, K.; Okamoto, K. *Jpn. J. Appl. Phys.* **1993**, *32*, 1523.
(30) Kayser, O. *J. Cryst. Growth* **1991**, *107*, 989.

of desorption–readsorption steps along the non-growth surface to the growing film edge where they react. Because molecular collisions in the gas phase are responsible for the readsorption process, the mean free path of the gas-phase molecules must be sufficiently small in order to redirect the desorbing species back onto the non-growth surface. Alternatively, the growth species can diffuse along the non-growth surface. In both cases only those species with sufficient proximity impinge and decompose at the edge of the growth surface. Because Al encroachment was also found to occur on SiO_2 when wafers were exposed to DMEAA at much lower pressures (10^{-4}) Torr where the mean free path of the gas molecules ($\sim 10^1$ cm) was larger than the wafer dimension, no species undergoing desorption from SiO_2 could have been redirected onto the substrate surfaces. Surface diffusion is implicated as being responsible for the overgrowth.

Surface diffusion also leads to a significant reduction in the concentration of the growth species on the non-growth surface at the edges of the growth surface and result in a diminished nucleation rate in these areas.[31] The Al depletion regions illustrated in Figure 7 reflect the occurrence of this type of process. During the present study, however, we also observed examples of the opposite effect; higher Al particle densities on SiO_2 in the region bordering the metal surface.

Acknowledgment. This work was supported by the Center for Interfacial Engineering, a National Science Foundation Engineering Research Center. The authors would also like to thank Mark Romo at Rosemount Inc. for contributing some of the test patterns.

(31) Yamaguchi, K.; Ogasawara, M.; Okamoto, K. *J. Appl. Phys.* **1992**, *72*, 5919.